Locally-triggered hydrophobic collapse induces global interface self-cleaning in van-der-Waals heterostructures at room-temperature

2D Materials

OPEN ACCESS

RECEIVED
12 December 2019

REVISED
19 February 2020

ACCEPTED FOR PUBLICATION
3 March 2020

PUBLISHED
16 April 2020

PAPER

Locally-triggered hydrophobic collapse induces global interface self-cleaning in van-der-Waals heterostructures at room-temperature

Stefan Wakolbinger[1], Fabian R Geisenhof[1], Felix Winterer[1], Samuel Palmer[1,8], Juri G Crimmann[1], Kenji Watanabe[2], Takashi Taniguchi[2], Frank Trixler[3,4,5] and R Thomas Weitz[1,3,6,7]

[1] Physics of Nanosystems, Department of Physics, Ludwig-Maximilians-Universität München, Amalienstrasse 54, Munich 80799, Germany
[2] National Institute for Materials Science, Tsukuba, Japan
[3] Center for Nanoscience (CeNS), Schellingstr. 4, Munich 80799, Germany
[4] Department of Earth and Environmental Sciences, Ludwig-Maximilians-Universität München, Theresienstraße 41, München 80333, Germany
[5] TUM School of Education, Technical University of Munich and Deutsches Museum, Museumsinsel 1, München 80538, Germany
[6] Munich Center for Quantum Science and Technology (MCQST), Schellingstrasse 4, Munich 80799, Germany
[7] 1st Physical Institute, Faculty of Physics, University of Göttingen, Friedrich-Hund-Platz 1, Göttingen 37077, Germany

E-mail: Thomas.weitz@lmu.de

Keywords: van-der Waals materials, interface manipulation, atomic force microscopy, heterostructure, self-cleaning

Supplementary material for this article is available online

Abstract

Mutual relative orientation and well defined, uncontaminated interfaces are the key to obtain van-der-Waals heterostacks with defined properties. Even though the van-der-Waals forces are known to promote the 'self-cleaning' of interfaces, residue from the stamping process, which is often found to be trapped between the heterostructure constituents, can interrupt the interlayer interaction and therefore the coupling. Established interfacial cleaning methods usually involve high-temperature steps, which are in turn known to lead to uncontrolled rotations of layers within fragile heterostructures. Here, we present an alternative method feasible at room temperature. Using the tip of an atomic force microscope (AFM), we locally control the activation of interlayer attractive forces, resulting in the global removal of contaminants from the interface (i.e. the contaminants are also removed in regions several μm away from the line touched by the AFM tip). By testing combinations of various hydrophobic van-der-Waals materials, mild temperature treatments, and by observing the temporal evolution of the contaminant removal process, we identify that the AFM tip triggers a dewetting-induced hydrophobic collapse and the van-der-Waals interaction is driving the cleaning process. We anticipate that this process is at the heart of the known 'self-cleaning' mechanism. Our technique can be utilized to controllably establish interlayer close coupling between a stack of van-der-Waals layers, and additionally allows to pattern and manipulate heterostructures locally for example to confine material into nanoscopic pockets between two van-der-Waals materials.

The combination of van-der-Waals (vdW) materials to heterostructures has boosted their overall quality on the one side and breadth of functionality for their possible application on the other [1]. The field became even more exciting, when also the rotational degree of freedom between the crystal lattices in a heterostructure could be controlled, peaking with the tuneability of electronic properties in twisted bilayer graphene and the discovery of unconventional superconductivity in 'magic angle' graphene bilayers [2–4]. In realizing such fragile systems, the quality of vdW heterostructures has benefited from the so-called 'self-cleaning' process [5, 6] that stems from the mutual vdW interactions between adjacent vdW

[8] Current address: School of Physics and Astronomy, The University of Nottingham, University Park, Nottingham NG7 2RD, UK

materials and has been attributed to the removal of interfacial contaminants. Even though this phenomenology is accepted, its microscopic temporal evolution has up to now not been visualized and additionally for reliable sample preparation, challenges like the contamination of interfaces with residual material from the transfer process [1, 5, 6] and precise and controlled relative positioning of the 2D-sheets [3, 4] remain. For example, while state of the art methods to facilitate clean interfaces can be performed at temperatures below 70 °C [6], others use a high temperature annealing step to aid self-cleaning or are performed at elevated temperatures [7, 8]. However, excess thermal energy is known to induce changes in relative crystallographic orientation [9, 10] or strain variations [11]. It follows naturally, that adding more knowledge on underlying mechanisms for low-temperature cleaning is desirable. Alternative cleaning methods that do not involve annealing use an atomic-force microscopy (AFM) tip to push material on top of vdW layers [12] or between vdW heterostacks [13] away from the areas of interest. In these methods, the vdW layers are only cleaned in the regions touched by the AFM tip.

Motivated understand and visualize the self-cleaning properties of vdW heterostructures at the nanoscale on the one side, and to develop an alternative cleaning method that can preserve the mutual angular alignment of adjacent vdW layers during the assembly process and still ensure clean interfaces on the other, we have developed systematics, that allow to remove residual contaminants between two vdW materials at ambient temperatures. Our method is triggered by the force exerted by an AFM tip which we control to locally bring two vdW layers separated by a layer of contaminants into immediate contact (see figure 1(a)). This local contact leads to a dewetting-induced hydrophobic collapse of regions adjacent to the close contact area. The expansion of these regions of immediate vdW contact extend over several μm into regions that had not been indented by the AFM tip, accompanied by the removal of contaminants between the layers. Our process is thus distinct from previous AFM cleaning methods in which the AFM tip had to be rastered across the entire region in which the contaminants were removed [12, 13]. Such methods might however lead to movement of e.g. domain boundaries in vdW multilayers [14]. An important advantage of our method, is its effectiveness at room temperature, where vdW materials were found to not rotate against one another.

The samples are prepared by exfoliation [15] of 2D materials onto a silicon wafer covered with 300 nm of SiO_2, as well as onto a PDMS covered glass slide. Suitable flakes are chosen using optical microscopy, and Raman-spectroscopy is conducted to determine the layer number and stacking order [16]. The h-BN was synthesized as reported in [17] and exfoliated directly onto SiO_2 substrates. The detailed morphology of the respective substrate surface is characterized with an AFM prior to the transfer step. The characterized 2D-materials are then combined to a heterostructure following the 'all-dry viscoelastic stamping method' in ambient air as described in [18]. Samples that we have prepared in this manner display residual material trapped between the two vdW layers, which is most probably adsorbed hydrocarbons and water [1, 5] that has been collected on the surfaces of the vdW materials in the time between exfoliation and stamping. An AFM image of an actual heterostructure composed of a bilayer graphene (2LG) stamped across three as-exfoliated flakes, a monolayer graphene flake (1LG, the crossing point is called interface 1), a 2LG (interface 2) and a trilayer graphene (3LG, interface 3) is shown in figure 1(b). Directly after the stamping process, the vdW materials are separated by approximately 5 nm of residual material (see inset to figure 1(b)).

To bring the materials into close contact, we have moved an AFM tip in contact mode for 500 nm across the interfacial region 3 (indicated as white dotted line in figure 1(b)). This process is called scratching in the remainder of the manuscript (please note that the surface is not damaged by this process). The tip pushes the transferred flake towards the lower flake, and it is reasonable to assume that close contact with significant van-der-Waals interaction between the 2D materials is thus initiated along the scratched path. In parallel, the trapped material is expelled from the manipulated area. We found, that if we image the same area directly after the scratch had been performed, the region of close contact had expanded significantly beyond the simple one-dimensional scratch made initially (figure 1(c)). We note, that the AFM images are taken during the expansion of the region of close vdW contact, so that each line-scan of the image captures the status of the expansion process at different state of the process (images are all taken from top to bottom and the time is indicated next to the images). Furthermore, normal tapping-mode imaging does not lead to regions of close contact—i.e. only when we purposely use the contact mode, material between the layers can be expelled. It is apparent that once an initial nucleus of close vdW contact between upper and lower layer has been established, attraction along the edges of already cleaned areas pull the sheets further together and promote the expansion of the close contact area far beyond the scratch path (i.e. what we are visualizing is the self-cleaning process of vdW heterostructures as detailed below). It should be emphasized, that the scratch was conducted at 21 °C and no high temperature steps were involved. We have repeated the scratching also at the interface region 2, where we have brought the stamped 2LG in close contact with the underlying 2LG, again

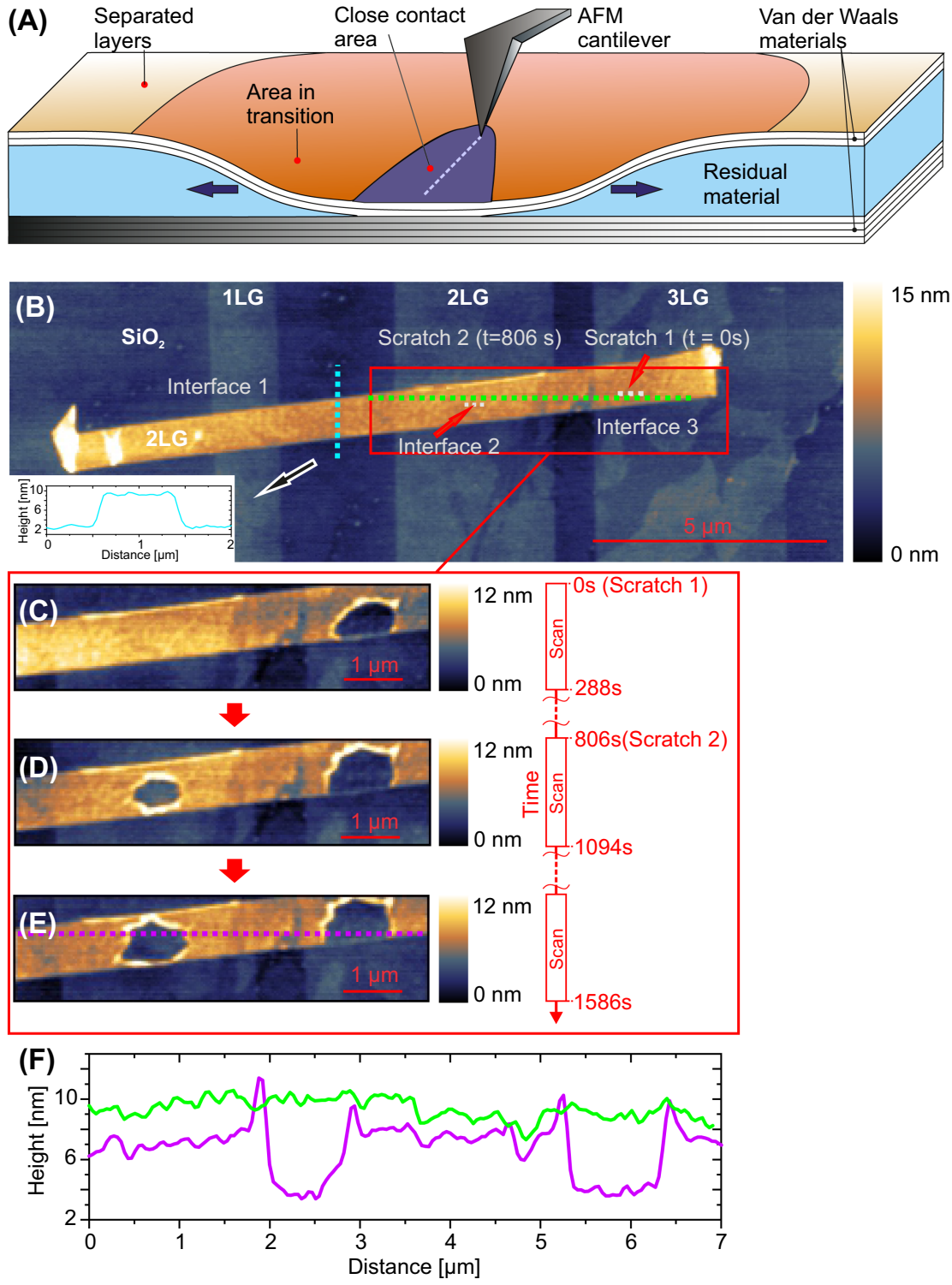

Figure 1. (a) Schematic of our interface cleaning method using local AFM indentation. (b) AFM-image of three heterostructures, where the top and lower vdW materials are seperated by a layer of contaminants. Inset: cross section along the turquoise line. (c), (d) Evolution of interface 3 (2), 288 s after it had been scratched. (e) Interface 3, 1586 s and interface 2 760 s after the respective close contact had been established. The cleaned area spreads far beyond the initial scratch-path. Manipulation of all interfaces was conducted at 21 °C and an overview of when the scratches are performed and when the respective images are finished can be seen in the time axis on the right side of the AFM images. (f) AFM linecuts before (from (b)) and after (from (e)) close contact has been initiated.

via a scratch indicated by the white dotted line in figure 1(b). The resulting AFM image can be seen in figure 1(d) directly after the second scratch was performed and again an expanding region of close contact can be seen. The linecut in figure 1(f) also shows this change in distance between the two vdW sheets upon establishment of close contact.

Besides AFM imaging, we have also utilized Raman spectroscopy to determine the degree of interlayer coupling pre and post cleaning. An example

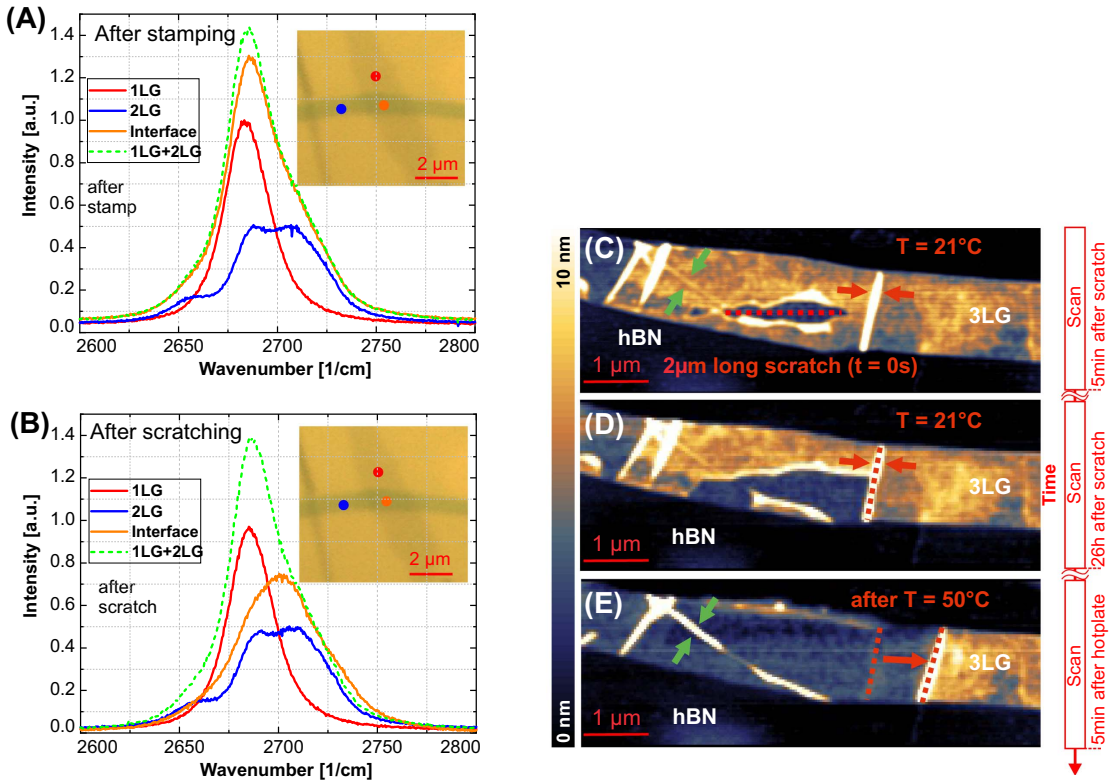

Figure 2. 2D-Raman modes before (a) and after (b) close contact is established at the interface between a 1LG (red solid), stamped 2LG (blue solid) and the resulting interface (orange solid). The sum-signal of the 1LG and 2LG is shown in both cases as a reference to the interface signal. To reach homogeneous cleaning we performed several scratches and anneald at 50 °C and subsequently at 80° (see discussion in text). Optical image of the stamped flakes are given in the insets to (a) and (b). (c)–(e): AFM images of a three layer graphene sheet on a hBN substrate. A scratch is performed along the red dotted line shown in (c), leading to a self-spreading cleaning process in the vicinity of the scratch. (d) Evolution of the clean area 26 h after the scratch and storage at T = 21°C in ambient air. (e) The same stack after 5 min on a hotplate at 50 °C, upon which the region of intimate vdW contact has extended rapidly.

of a stamped 1LG/2LG heterostructure is shown in figures 2(a) and (b). Figure 2(a) shows the 2D mode in the interface (orange) before manipulation as well as the 2D mode of the 1LG (red) and 2LG (blue) next to the interface. The green dashed line corresponds to the summed signal of the 1LG and the 2LG. It is almost identical to the orange trace recorded in the interface area, indicating that the latter signal is purely a superposition of the signals of the two individual flakes. This leads us to conclude, that there is no direct interaction between the layers directly after the stamping process, and the residue trapped at the interface acts as spacer between the sheets inhibiting coupling of phonon modes. After bringing the two layers in close contact employing our method as described before, the resulting Raman signal (see figure 2(b)) of the heterostructure has changed significantly. The most important changes are the huge decrease of the interface signal intensity and a shift of the peaks maximum from 2688 cm^{-1} to 2701 cm^{-1} as well as an increase of the full-width at half maximum (FWHM). The peak position, signal intensity and FWHM have a strong similarity to the signal of 3LG in previous work [16, 19] implying that strong interlayer coupling could be established after the manipulation. For further Raman spectroscopy results showing the same phenomenology in different heterostructures see figure S4 (stacks.iop.org/2DM/7/035002/mmedia) in the SI.

Apart from graphene, the AFM-induced removal of contaminants between stamped layers works as well in a combination of other vdW materials, for example when graphene or its multilayers are stamped onto hexagonal Boron Nitride (hBN) or Molybdenum Disulfide (MoS_2). More generally speaking, we anticipate, that our method will work in all vdW materials in which also high-temperature annealing works [5, 7] (whereas the latter process might lead to mutual rotations of the layers). As an example, figure 2(c) shows a 3LG flake stamped onto multilayer hBN, which has been subsequently scratched along a 2 μm long line. Already after five minutes a significantly expanded region of close contact can be seen. A further example of a graphene—MoS_2 interface is shown in figures S1 and S2 in the supplementary information. Our method did not work when one of the partners is a non-vdW material, e.g. when multilayer graphene is stamped onto gold contacts or a SiO_2 substrate.

After studying the interaction between the vdW layers before and after initiating close contact, we turn towards the investigation of the mechanism driving the non-local cleaning process. The speed at which

the region of close contact propagates, seems to differ in samples where various layer numbers have been used to form the heterostructure, and—compared to other annealing methods—we benefit from the slow expansion and are thus able to gradually visualize it in different stages of the process. For example, the 2LG-2LG and 3LG-2LG interface in figure 1 are easily brought in close contact by a simple 1D-AFM scratch and storage at room temperature for few minutes, whereas the 3LG-2LG interface proceeds slightly faster. In contrast, in the 1L-2LG interface (interface 1) the region of close contact after scratching spreads very slowly across the sample at room temperature even though we also had performed a scratch in interface 1 (see figure S3 for corresponding AFM images—the region of close contact has not spread notably 10 min after the scratch had been performed). The experimental data suggests a scaling and thus a higher effectivity (defined as further expanding of the close contact area within the same amount of time passed after the scratch) for the cleaning process with increasing layer thickness. Besides other factors, this seems to be related to a stronger vdW coupling and higher hydrophobicity between the vdW sheets [20] with increasing layer number. The quantification of the Hamaker coefficient [21] and scaling laws for vdW interaction [22] are in agreement with our observation. Additional experiments showing how scaling the vdW interaction changes the speed of the interface cleaning is shown in figure S4, where we have stamped a 2LG onto a 1LG located on SiO_2 and in a separate stamping run a 1LG onto a 2LG located on SiO_2. The interfacial cleaning is significantly faster in the case, that the 2LG is located on the SiO_2, which can be explained by the wetting transparency or translucency of graphene [23–25]. In other words the hydrophilic SiO_2 weakens the vdW interactions of 1LG more significantly than in 2LG, as reported previously [23]. Finally, we also found a single outlier to this trend which was consistent in the other 11 investigated graphene heterostacks (21 interfaces in total were investigated) as shown in figure S5. Here, even though a 1LG had been stamped onto a 2LG, the spreading of the region of close contact did not proceed quickly, the cause of which is currently unclear, suggesting that also other parameters than hydrophobicity and vdW strength might contribute to the efficiency of the process.

The attractive vdW forces—even in the case when thick layers are used—are typically not strong enough to clean the entire interfacial region. It is reasonable to assume, that during the process a counteracting force builds up, which eventually hinders the process. This force most probably originates from the increasing amount of material redistributed from the area of close contact and now accumulating in a fold adjacent to it, which needs to be pushed from the interface region to enable cleaning [7]. An example is shown in figures 2(c)–(e), where 26 h after bringing a 3LG flake in close contact with an underlying h-BN flake, the expansion of the close contact area has stopped (see figure 2(b)). Here, also the region of accumulated materials can be seen (for a more detailed image see figure S6 in the SI). As shown in figure 2(e), the close contact area continues to grow after an increase of temperature to 50 °C for 5 min, a temperature that is usually too low to remove residual material between flakes in the case that no region of close contact has been established prior to heating (see e.g. figure 2(e)—in the very right part of the flake no region of close contact has been initiated after the 50 °C annealing step). It is apparent from figure 2 that only in the case that intimate vdW contact has been established a very low annealing temperatures of 50 °C, can support the rapid removal of residual material between the layers within few minutes (and additionally can move the large fold visible in the right section of the Flake in figures 2(c)–(e).

Finally, we note that there are folds visible in figures 2(c)–(e) prior to and after cleaning. These do not stem from the AFM-induced cleaning itself, but are present prior to the cleaning process and stem for example from the stamping. Two examples of such wrinkles are marked in figures 2(c)–(e) with green and red arrows. The wrinkles are moved by mild temperature treatment (compare figures 2(d) and (e)) in some instances.

While the general phenomenology that the vdW interaction leads to self-cleaning is known [1, 5, 7, 26], we can now add more systematics to this phenomenon. Furthermore, from the observed dependencies of the cleaning process on the type of substrate, the thickness of the vdW layers and the temperature we can detail the underlying mechanism that leads to the spreading of the region of close contact. According to our observations interface cleaning and spreading only occurs when vdW materials such as graphene [20, 27], MoS_2 [28], or hBN [29] are combined. Furthermore, we note that along with the vdW character of the mentioned materials, the material's partner must also be hydrophobic for interfacial cleaning to occur, since if one of the partners is hydrophilic and not a vdW material as in the case of gold [30] and SiO_2 [31], no interface cleaning can be detected. A correlation of interface cleaning with hydrophobicity is further supported by the fact that e.g. 2LG is more hydrophobic than 1LG [20]. This coincides with our observation that after inducing an intimate local contact via AFM an expansion of the area of close contact does not occur at the same rate in the 1LG/2LG interface (in the case that the 1LG is located directly on the SiO_2) while a 2LG/2LG interface shows fast expansion (spreading). These correlations indicate that hydrophobicity is in addition to the vdW character an important parameter for interface cleaning and spreading dynamics, of which both factors will be discussed in further detail below.

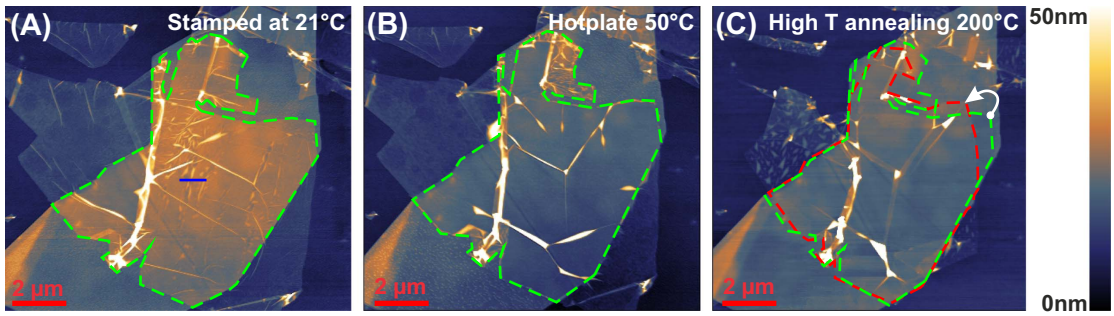

Figure 3. AFM images of a two layer graphene sheet on a hBN substrate. (a) Heterostructure with the interface indicated as green dashed area directly after dry transfer. The interface cleaning was initiated along the scratch path, indicated as blue solid line. (b) Heterostructure after the scratch and additionally 5 min at 50 °C on a hotplate. Most of the material in the interface is removed and the relative position of the flakes remains unchanged. (c) Interface after 2 h at 200 °C in the vacuum-oven. The 2LG has undergone significant rotation and translation. The new interface is indicated as red dashed area.

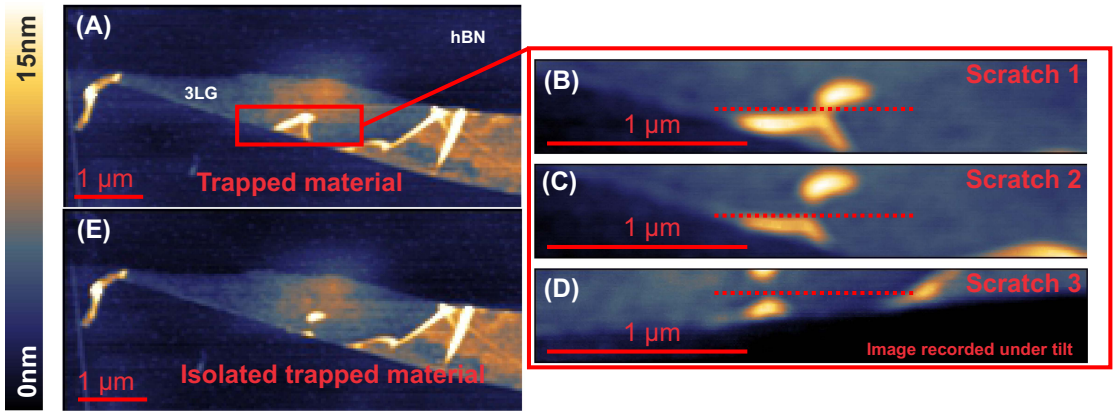

Figure 4. AFM images of a three layer graphene flake on a mutilayer hBN substrate. This is the same flake as shown in figure 2, images were taken however prior to the investigations discussed in figure 2. A partially clean interface can be seen in (a), where residual material accumulates in a reservoir at the edge of the interface. (b) A portion of the residue is cut off by scratch 1, and the rest of the material is removed from the interface by scratch 2 and 3(c)–(e) Nanoscopic region of confined material after manipulation.

Having described above our experimental observation that increasing thickness and consequently strength of the vdW interaction increases the efficiency of the self-cleaning, we now discuss how the hydrophobicity plays a role in this process. We propose that dewetting induced hydrophobic collapse [32]—an effect which is of high importance e.g. in molecular biology [33] and nanofluidics [34]—plays a central role in the observed removal of water from the interface of vdW heterostructures. In general, the effect describes an aggregation phenomenon (collapse) of dispersed solid hydrophobes driven by the expulsion (dewetting) of hydrophilic liquids between them. The cause of this phenomenon is a non-classical behaviour of polar liquids such as water when confined between two hydrophobic surfaces at nanoscale distances [35]. Various simulations performed with two opposing, nm-sized confining planar surfaces in a water bath have indicated, that at ambient conditions nano-confined liquid water becomes metastable to its vapour state below a critical distance of the confining surfaces [36, 37]. According to these calculations, the close distance leads to a depletion of water between the hydrophobic surfaces [32, 35–37]. Such a dewetting transition (evaporation) precede a hydrophobic collapse which results in a direct stacking of the two surfaces [32]. In terms of dewetting kinetics within hydrophobic nanoconfinements there is a linear scaling of the free energy barrier $\Delta G/kT$ (to nucleate an evaporation event) with the distance (gap size) [37]. Such a nucleation barrier decreases with lower gap size. This is due to thermal fluctuations in the shape of vapour pockets between hydrophobic surfaces which reduce the activation barrier significantly [36]. The critical distance for evaporation increases with increasing hydrophobicity [32] as well as with increasing temperature [38] while the evaporation rate increases with decreasing distance of the surface plates [37]. Our experimental observations are in good agreement with the described dewetting-induced hydrophobic collapse phenomenology, which shows a strong dependency on the distance of the surface plates and also scales its efficiency with the hydrophobicity degree of the confining plates: In our experiments, a local decrease of the separation of graphene sheets via the force exerted

by an AFM tip towards the critical distance induces evaporation transitions of nano-confined water as the nucleation barrier decreases. This leads to a depletion (drying) and enables interlayer coupling of the vdW layers via hydrophobic collapse. Increasing hydrophobicity via increasing the number of graphene layers (from 1LG to 2LG to 3LG) raises the critical distance (i.e. makes the cleaning process more efficient). This allows evaporation of confined water at larger gap sizes. Increasing temperature also raises the critical distance. As the evaporation rate increases with lower distance or—from the perspective of constant separation—with raised critical distance, spreading of close contacts is therefore enhanced at higher temperatures. In other words, we anticipate that in our experiments the AFM tip acts as initiator for a local nucleus of reduced distance of the two vdW materials resulting in subsequent hydrophobic collapse at that location and the adjacent area. This leads to the observed large scale transverse transfer of confined water away from the region of AFM interaction and thus enhances subsequent drying transitions and dewetting induced hydrophobic collapse.

While water layers on a graphene surface have a steric repulsive contribution to the self-assembling properties of parallel graphene sheets and can create a metastable separation [39], our proposed model indicates that the forced interlayer distance reduction by the AFM tip below a critical distance apparently creates a condition favoring dewetting induced hydrophobic collapse of this metastable separation. This condition removes confined water layers (and with it we assume the potentially also present hydrocarbons) and creates an attractive force allowing the sheets to approach to each other. After reaching a second critical distance (which depends on the Hamaker coefficient) the Lennard-Jones potential of the interaction between the upper and the lower layers becomes significantly attractive [39] so the resulting vdW forces generate inter-layer coupling in 2D vdW heterostructures. This forms a nucleus of close vdW contact.

The area in transition between the nucleus of close vdW contact and the separated layers forms an ascending slope with a gradient in the order of about 0.15–0.20 [40]. Due to this low gradient a segment of the ascending slope can extend up to several nm laterally before it vertically crosses the respective critical distance for dewetting induced hydrophobic collapse (which is in the order of about 1.2 nm at 300 K for two free-standing graphene layers dispersed in water [41]). As a consequence, this segment can also undergo hydrophobic collapse and inter-layer coupling which subsequently pulls also the adjacent segment below the two critical distances. This creates a front of hydrophobic collapse and inter-layer coupling, which propagates increasingly away from the initial nucleus of close contact.

Our method is distinct from previously used high-temperature methods for removal of contaminants [7] since it does not induce mutual rotations of the stamped layers, as is the case of high-temperature cleaning methods [10]. As an example, we have stamped a 2LG layer onto a multilayer hBN flake. The resulting heterostructure is shown in figure 3(a). The interface is scratched along the blue line and subsequently annealed at 50 °C for 5 min to speed up the cleaning process. The result is a nearly complete interface cleaning as illustrated in figure 3(b). It is worth emphasizing, that the flake did not rotate or shift relative to the hBN substrate. An additional annealing step at 200 °C for 2 h in a vacuum is conducted in order to investigate reorientation effects in the same sample caused by higher temperatures. The resulting position of the flake on the hBN substrate is indicated by the red dashed area in figure 3(c). The 2LG flake translates several hundred nanometres to the left as well as rotates relative to the hBN substrate. Further examples of flakes, which have been treated with the same protocol and show the same phenomenology, are shown in supplementary figure S7. These observations indicate that rotations, which would occur in a heterostructure at high temperatures, can be avoided and clean interfaces can be achieved easily with our method.

Besides the possibility of bringing two vdW materials in close contact without mutual rotation, our technique also allows the creation of encapsulated pockets containing the residual material contained between the two vdW materials. To illustrate this, we have performed an experiment where we manipulate a pocket with trapped material in order to separate the encapsulated material in two reservoirs (figure 4). Part of the material is subsequently removed from the interface by several 1 μm long scratches shown in figures 4(c)–(d). The resulting nano-bubble in figure 4 is about 300 nm in diameter and 9 nm in height, similar to reported sizes of enclosed regions which however had not been formed deliberately [42]. Our method is especially suitable to create deterministically shaped confined pockets, since we can choose conditions at which the spreading process proceeds on an hour timescale, as shown in figures S4(d)–(f). Such pockets might be interesting to study for example nano-confined water [43] or biomolecules in water in confined spaces [44].

Conclusion

We have investigated in great microscopic detail the self-cleaning mechanism between vdW layers and devised a straightforward method to bring functional 2D layers separated by a layer of contaminants into close contact. Our method does not rely on an increase in temperature, but only on interlayer attractive van-der-Waals forces and the hydrophobic

nature of the materials, which leads to a dewetting induced hydrophobic collapse. Distinct from previous investigations [7] that have examined the systematics of mobility of trapped materials at elevated temperatures in stacks already in close vdW contacts, we have elucidated the initial stages of vdW self-cleaning. With our method we can realize clean van-der-Waals heterostructures without high-temperature annealing steps (which are known to induce mutual rotation of the used materials) and we therefore anticipate that our method can be especially helpful to create clean van-der-Waals stacks in the case that the control of mutual layer rotation is a concern. Having said that, using our method we were only able to create up to 10 μm [2] large clean areas, whereas especially high-temperature methods are able to create clean vdW heterostructures that are essentially as large as the vdW structures itself [7]. Additionally, the slow nature and consequently high controllability of our technique can be used to pattern interfaces such as artificially formed nano-bubbles.

Methods

All graphene flakes which were stamped were directly exfoliated onto PDMS stamps and subsequently transferred to target flakes (which in turn had been exfoliated directly onto the SiO_2 (300 nm)/Si wafers) using the 'all-dry viscoelastic stamping method' in ambient air as described in [18]. AFM manipulation and scanning was performed with a Vecco Digital Instruments Nanoscope and Nanoscope IIIa (as force mode controller). The cantilevers were a silicon tips from Asylum Research Oxford Instruments Model AC160TS tapping tips with spring constants of ~26 N m^{-1} and a tip diameter of 7 nm and a symmetric shape with a cone half-angle of 9 degrees or less. Tip sensitivity has been measured prior to measurement by pressing onto a SiO_2 substrate. We have then slowly performed multiple lines of indent with increasing force starting from forces of about 10 nN to identify the threshold of close contact. After each line of indent, we have imaged the indented position in tapping mode to identify if close contact (visible for example in figure 1(c)) has been established. In the case that no close contact had been established, we have increased the force and performed a line of ident in the contact mode. The threshold upon which close contact can be established depends mainly on the position on the sample namely if the scratch starts at a bubble or a relatively non-polluted area. We have found, that close contact can be initiated by nano-indentation of varying applied forces from 1124 nN for indentation on a bubble to 80 nN on a relatively clean position. Following this protocol of slowly increasing the force used while scratching until close contacts was initiated, more than 90% of the investigated heterostructures could be brought in close contact. In the case that successful contacts could be established, we did not find that the tip was damaged by the scratch. We also note, that the applied force needs to be kept as small as possible (i.e. just enough to initiate contact), since in the case that the two layers are indented beyond the point of close contact they might be damaged. Our method to determine integrity of the scratched flakes was AFM, SNOM and Raman where we could not find evidence of any damage caused by the AFM tip in the majority of the samples. Although we want to emphasize that the interacting force of an AFM in scratch and tapping mode can be increased until the tip eventually damages the surface, so a heterostructure can be damaged if the (interaction) scratch is too strong (i.e. significantly larger than the force required to initiate close contact). All scratches were performed at 21 °C in ambient air. The annealing cycle for high temperature annealing in vacuum involved the steps: Firstly, a ramp up to 200 °C in 2 h, secondly, an annealing step for 30 min and finally a ramp down to 21 °C in 2 h. The Raman measurements have been performed in a Horiba system (T64000) at 514 nm laser excitation wavelength.

Acknowledgment

R T W acknowledges funding from the excellence initiative Nanosystems Initiative Munich (NIM), the Center for Nanoscience (CeNS) and the Solar Technologies go Hybrid (SolTech) initiative. We additionally acknowledge funding by the Deutsche Forschungsgemeinschaft (DFG, German Research Foundation) under Germany's Excellence Strategy – 'EXC-2111– 390814868 (MCQST) and EXC 2089 /1 –390776260.' (e-conversion). We also acknowledge Jochen Feldmann for using his Raman setup. K W and T T acknowledge support from the Elemental Strategy Initiative conducted by the MEXT, Japan, A3 Foresight by JSPS and the CREST (JPMJCR15F3), JST.

ORCID iDs

Stefan Wakolbinger https://orcid.org/0000-0002-3194-3402
Fabian R Geisenhof https://orcid.org/0000-0002-3623-1906
Kenji Watanabe https://orcid.org/0000-0003-3701-8119
R Thomas Weitz https://orcid.org/0000-0001-5404-7355

References

[1] Geim A K and Grigorieva I V 2013 Van der Waals heterostructures *Nature* **499** 419–25

[2] Jorio A and Cançado L G 2013 Raman spectroscopy of twisted bilayer graphene *Solid State Commun.* **175–176** 3–12
[3] Ribeiro-Palau R, Zhang C, Watanabe K, Taniguchi T, Hone J and Dean C R 2018 Twistable electronics with dynamically rotatable heterostructures *Science* **361** 690–3
[4] Cao Y, Fatemi V, Fang S, Watanabe K, Taniguchi T, Kaxiras E and Jarillo-Herrero P 2018 Unconventional superconductivity in magic-angle graphene superlattices *Nature* **556** 43–50
[5] Haigh S J, Gholinia A, Jalil R, Romani S, Britnell L, Elias D C, Novoselov K S, Ponomarenko L A, Geim A K and Gorbachev R 2012 Cross-sectional imaging of individual layers and buried interfaces of graphene-based heterostructures and superlattices *Nat. Mater.* **11** 764–7
[6] Kretinin A V, Cao Y, Tu J S, Yu G L, Jalil R, Novoselov K S, Haigh S J, Gholinia A, Mishchenko A Lozada M *et al* 2014 Electronic properties of graphene encapsulated with different two-dimensional atomic crystals *Nano Lett.* **14** 3270–6
[7] Purdie D G, Pugno N M, Taniguchi T, Watanabe K, Ferrari A C and Lombardo A 2018 Cleaning interfaces in layered materials heterostructures *Nat. Commun.* **9** 5387
[8] Jain A, Bharadwaj P, Heeg S, Parzefall M, Taniguchi T, Watanabe K and Novotny L 2018 Minimizing residues and strain in 2D materials transferred from PDMS *Nanotechnology* **29** 265203
[9] Sinclair R C, Suter J L and Coveney P V 2018 Graphene-graphene interactions: friction, superlubricity, and exfoliation *Adv. Mater.* **30** e1705791
[10] Wang D, Chen G, Li C, Cheng M, Yang W, Wu S, Xie G, Zhang J, Zhao J Lu X *et al* 2016 Thermally induced graphene rotation on hexagonal boron nitride *Phys. Rev. Lett.* **116** 126101
[11] Woods C R, Withers F, Zhu M J, Cao Y, Yu G, Kozikov A, Ben Shalom M, Morozov S V, van Wijk M M Fasolino A *et al* 2016 Macroscopic self-reorientation of interacting two-dimensional crystals *Nat. Commun.* **7** 10800
[12] Goossens A M, Calado V E, Barreiro A, Watanabe K, Taniguchi T and Vandersypen L M K 2012 Mechanical cleaning of graphene *Appl. Phys. Lett.* **100** 73110
[13] Rosenberger M R, Chuang H-J, McCreary K M, Hanbicki A T, Sivaram S V and Jonker B T 2018 Nano-'Squeegee' for the creation of clean 2D material interfaces *ACS Appl. Mater. Interfaces* **10** 10379–87
[14] Jiang L, Wang S, Shi Z, Jin C, Utama M I B, Zhao S, Shen Y-R, Gao H-J, Zhang G and Wang F 2018 Manipulation of domain-wall solitons in bi- and trilayer graphene *Nat. Nanotechnol.* **13** 204–8
[15] Novoselov K S, Geim A K, Morozov S V, Jiang D, Zhang Y, Dubonos S V, Grigorieva I V and Firsov A A 2004 Electric field effect in atomically thin carbon films *Science* **306** 666–9
[16] Nguyen T A, Lee J-U, Yoon D and Cheong H 2014 Excitation energy dependent Raman signatures of ABA- and ABC-stacked few-layer graphene *Sci. Rep.* **4** 4630
[17] Taniguchi T and Watanabe K 2007 Synthesis of high-purity boron nitride single crystals under high pressure by using Ba–BN solvent *J. Cryst. Growth.* **303** 525–9
[18] Castellanos-Gomez A, Buscema M, Molenaar R, Singh V, Janssen L, van der Zant H S J and Steele G A 2014 Deterministic transfer of two-dimensional materials by all-dry viscoelastic stamping *2D Mater.* **1** 011002
[19] Geisenhof F R, Winterer F, Wakolbinger S, Gokus T D, Durmaz Y C, Priesack D, Lenz J, Keilmann F, Watanabe K Taniguchi T *et al* 2019 Anisotropic strain-induced soliton movement changes stacking order and band structure of graphene multilayers: implications for charge transport *ACS Appl. Nano Mater.* **2** 6067–75
[20] Munz M, Giusca C E, Myers-Ward R L, Gaskill D K and Kazakova O 2015 Thickness-dependent hydrophobicity of epitaxial graphene *ACS Nano* **9** 8401–11
[21] Chiou Y-C, Olukan T A, Almahri M A, Apostoleris H, Chiu C H, Lai C-Y, Lu J-Y, Santos S, Almansouri I and Chiesa M 2018 Direct measurement of the magnitude of the van der waals interaction of single and multilayer graphene *Langmuir: ACS J. Surf. Colloids* **34** 12335–43
[22] Gobre V V and Tkatchenko A 2013 Scaling laws for van der Waals interactions in nanostructured materials *Nat. Commun.* **4** 2341
[23] Rafiee J, Mi X, Gullapalli H, Thomas A V, Yavari F, Shi Y, Ajayan P M and Koratkar N A 2012 Wetting transparency of graphene *Nat. Mater.* **11** 217–22
[24] Shih C-J, Strano M S and Blankschtein D 2013 Wetting translucency of graphene *Nat. Mater.* **12** 866–9
[25] Belyaeva L A, van Deursen P M G, Barbetsea K I and Schneider G F 2018 Hydrophilicity of graphene in water through transparency to polar and dispersive interactions *Adv. Mater.* **30** 1703274
[26] Sun J-S, Jiang J-W, Park H S and Zhang S 2017 Self-cleaning by harnessing wrinkles in two-dimensional layered crystals *Nanoscale* **10** 312–18
[27] Leenaerts O, Partoens B and Peeters F M 2009 Water on graphene: hydrophobicity and dipole moment using density functional theory *Phys. Rev.* B **79** 10.1103/PhysRevB.79.235440
[28] Bampoulis P, Teernstra V J, Lohse D, Zandvliet H J W and Poelsema B 2016 Hydrophobic Ice confined between graphene and MoS 2 *J. Phys. Chem.* C **120** 27079–84
[29] İlhan B, Kurt M and Ertürk H 2016 Experimental investigation of heat transfer enhancement and viscosity change of hBN nanofluids *Exp. Therm. Fluid Sci.* **77** 272–83
[30] Smith T 1980 The hydrophilic nature of a clean gold surface *J. Colloid Interface Sci.* **75** 51–55
[31] Zorba V, Persano L, Pisignano D, Athanassiou A, Stratakis E, Cingolani R, Tzanetakis P and Fotakis C 2006 Making silicon hydrophobic: wettability control by two-lengthscale simultaneous patterning with femtosecond laser irradiation *Nanotechnology* **17** 3234–8
[32] Huang X, Margulis C J and Berne B J 2003 Dewetting-induced collapse of hydrophobic particles *Proc. Natl. Acad. Sci. U.S.A.* **100** 11953–8
[33] Young T, Hua L, Huang X, Abel R, Friesner R and Berne B J 2010 Dewetting transitions in protein cavities *Proteins* **78** 1856–69
[34] Qiu H, Zeng X C and Guo W 2015 Water in inhomogeneous nanoconfinement: coexistence of multilayered liquid and transition to Ice nanoribbons *ACS Nano* **9** 9877–84
[35] Remsing R C, Xi E, Vembanur S, Sharma S, Debenedetti P G, Garde S and Patel A J 2015 Pathways to dewetting in hydrophobic confinement *Proc. Natl. Acad. Sci. U.S.A.* **112** 8181–6
[36] Luzar A 2004 Activation barrier scaling for the spontaneous evaporation of confined water † *J. Phys. Chem.* B **108** 19859–66
[37] Sharma S and Debenedetti P G 2012 Evaporation rate of water in hydrophobic confinement *Proc. Natl. Acad. Sci. U.S.A.* **109** 4365–70
[38] Zangi R and Berne B J 2008 Temperature dependence of dimerization and dewetting of large-scale hydrophobes: a molecular dynamics study *J. Phys. Chem.* B **112** 8634–44
[39] Halim U, Zheng C R, Chen Y, Lin Z, Jiang S, Cheng R, Huang Y and Duan X 2013 A rational design of cosolvent exfoliation of layered materials by directly probing liquid-solid interaction *Nat. Commun.* **4** 2213
[40] Schniepp H C, Kudin K N, Li J-L, Prud'homme R K, Car R, Saville D A and Aksay I A 2008 Bending properties of single functionalized graphene sheets probed by atomic force microscopy *ACS Nano* **2** 2577–84
[41] Samanta T and Bagchi B 2018 Temperature effects on the hydrophobic force between two graphene-like surfaces in liquid water *J. Chem. Sci.* **130** 1
[42] Cheng M, Wang D, Sun Z, Zhao J, Yang R, Wang G, Yang W, Xie G, Zhang J Chen P *et al* 2014 A route toward digital

manipulation of water nanodroplets on surfaces *ACS Nano* **8** 3955–60

[43] Agrawal K V, Shimizu S, Drahushuk L W, Kilcoyne D and Strano M S 2017 Observation of extreme phase transition temperatures of water confined inside isolated carbon nanotubes *Nat. Nanotechnol.* **12** 267–73

[44] Khatib O, Wood J D, McLeod A S, Goldflam M D, Wagner M, Damhorst G L, Koepke J C, Doidge G P, Rangarajan A Bashir R *et al* 2015 Graphene-based platform for infrared near-field nanospectroscopy of water and biological materials in an aqueous environment *ACS Nano* **9** 7968–75